International Journal of Latest Research in Engineering and Technology (IJLRET)
ISSN: 2454-5031
www.ijlret.com || Volume 11 - Issue 08 || August 2025 || PP. 58-63

Loss and Efficiency Optimization Approach for Interleaved Switching Rectifier Circuits with AC Input based on Comprehensive Loss Analysis

Dr. Dongwoo Lee[1]
[1]*Assistant Professor, Department of Electrical & Control Engineering, Cheongju University, Korea*

Abstract: In this paper, a systematic method to improve losses and efficiency is proposed through loss and efficiency analysis of an interleaved switching rectifier circuit, which is one of the switching rectifier circuits with AC input. First, the current values of key components operating in steady state were classified into three proportional constants by weighting according to the load current, based on the basic circuit of the interleaved switching rectifier. Using these results, internal power losses related to load current can be analyzed. To verify the validity of the loss analysis, an experimental circuit for approximately 400W class interleaved switching rectifier was constructed and its results were compared with the theoretical calculations. The comparison showed that, across the entire load range, the theoretical and experimental values exhibited similar trends, indicating that the proposed approach can be effectively utilized in the actual design process.
Keywords: interleaved PFC, rectifier, efficiency analysis, power loss optimization

I. INTRODUCTION

In recent power devices utilizing alternating current (AC), miniaturization and high efficiency are considered critical design factors related to integration. In particular, rectifiers that convert AC to direct current (DC) face challenges in circuit design, as they must meet IEC61000-3-2 harmonic standards while ensuring cost competitiveness. Switching rectifiers used in power supplies that operate on AC require high-frequency switching to perform rectification and need to be controlled to generate low input current harmonic distortions. Power Factor Correction (PFC) circuits refer to switched rectifiers proposed to satisfy requirements such as rectification and reduction of harmonic currents, with various circuit topologies available considering power consumption, size, and manufacturing costs[1-4].

This study investigates loss analysis and improvements in power conversion efficiency during the design phase of interleaved switched rectifiers, aiming to enable optimal design with minimal losses. For efficient design, accurately analyzing power losses and minimizing them is essential. Specifically, predicting and considering loss factors precisely during the design stage allows for the optimization of component selection and circuit configuration, thereby enhancing overall system efficiency. Accordingly, this research analyzes the loss factors of key components within the rectifier and proposes strategies to optimize power conversion efficiency. It is anticipated that such analysis will enable product designers to determine optimal design parameters based on electrical characteristics and experimental data, leading to the development of high-efficiency interleaved switched rectifiers [5-8].

II. Interleaved Switched Rectifier

Fig. 1 illustrates the basic configuration of an interleaved rectifier circuit. Typically, an interleaved switching rectifier is an optimized structure designed to enhance the efficiency and performance of power conversion systems. It consists of multiple rectifier circuits arranged in parallel to overcome the limitations of traditional single-switching rectifiers. This architecture effectively reduces input current ripple and distributes switching losses, thereby improving overall system efficiency. The operating principle depicted in Fig. 1 involves a technique called interleaving, which intentionally phase-shifts the currents flowing through each inductor (L1, L2) when the input voltage (VIN) is applied. Switches (S1, S2) operate at a fixed switching frequency, adjusting the duty cycle to regulate the output voltage. By dispersing the switching instances of each switch, the circuit cancels out the input current ripple. Diodes (D1–D4) are synchronized with the switching operation to control current paths, while the output capacitor (C) performs voltage stabilization[9-11].

Fig. 2 presents waveforms of the input current and voltage, the currents through the two inductors, and the duty cycle of the two switches when the circuit operates under steady-state conditions with AC input. The inductor currents overlap, forming the total input current, which operates as a sine wave, thereby reducing the harmonic content of the input current.Fig.2 depicts the waveforms of key components observed during the operating steady-state in the switching cycle. From the top, it shows the control signals for the two switches, the currents through the two inductors, and the input current. In the Figure, the inductor currents exhibit a 180-

degree phase difference in accordance with their respective switch control signals, and it can be observed that the two inductor currents overlap. Since the current sharing occurs between the components, this enables efficient operation and contributes to improved reliability.

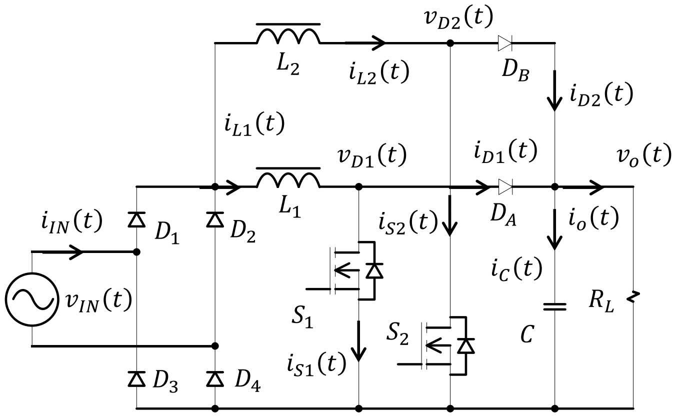

Fig.1: Basic circuit of interleaved PFC

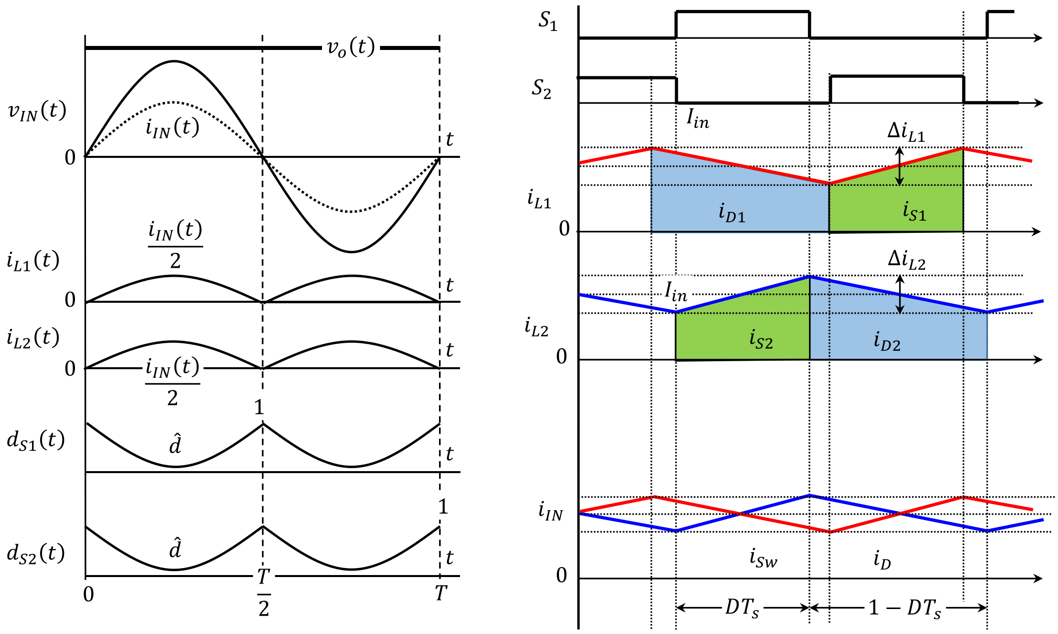

(a) Waveforms for AC input (b) Waveforms for switching cycle

Fig.2: Main operating waveforms in the steady state

III. The Root Mean Square (RMS) Current of the Key Components

Based on the basic circuit in Fig. 1 and the waveforms in Fig. 2, the RMS values of currents for the key components can be derived. It is possible to derive the root mean square (RMS) value of the current from the steady-state current waveform of the key components. The RMS current value is proportional to the load current, and each equation can be organized with the load current as a variable. The magnetic core that makes up the inductor experiences core losses as well as losses due to the current in the windings. The power loss in the core is related to the change in internal magnetic flux, and the magnetic flux is proportional to the load current. Table 1 classifies these load-current contributions into three categories, with proportional constants denoted accordingly. Specifically, the first term is independent of the load current, the second is proportional to the load current, and the third is proportional to the square of the load current.

Table 1: Power loss of the device reflecting the loss factor

Loss factor	Power loss	Equations
K_0	$P_{S(c)}$	$\frac{1}{2}\cdot V_o^2\cdot C_{oss}\cdot f_{sw}\cdot 2$
	$P_{D(j)}$	$\frac{1}{2}\cdot V_o^2\cdot C_D\cdot f_{sw}\cdot 2$
K_1	$P_{D(Drop)}$	$\frac{1}{2}\cdot V_F\cdot 2$
	$P_{B(Drop)}$	$\left(\frac{4\sqrt{2}\,V_o}{\pi V_{in(rms)}}\cdot V_{BF}\right)$
K_2	$P_{S(cond)}$	$\left(\frac{V_o}{\sqrt{2}V_{in(rms)}}\cdot\sqrt{1-\frac{8\sqrt{2}V_{in(rms)}}{3\pi V_o}}\right)^2\cdot R_{on}\cdot 2$
	$P_{D(cond)}$	$\left(\frac{V_o}{\sqrt{2}V_{in(rms)}}\cdot\sqrt{\frac{8\sqrt{2}}{3\pi}\frac{V_{in(rms)}}{V_o}}\right)^2 2r_L$
	$P_{L(cond)}$	$\left(\frac{V_o}{V_{in(rms)}}\right)^2\cdot r_L\cdot 2$
	$P_{L(core)}$	$\left(\frac{L}{A_eN}\cdot\frac{2\sqrt{2}\,V_o}{V_{in(rms)}}\right)^2\cdot f_{sw}^2\cdot V_e\cdot\frac{2}{\pi}$
	$P_{C(cond)}$	$\left(\frac{8\sqrt{2}\cdot V_o}{3\pi V_{in(rms)}}-1\right)\cdot R_{esr}$

IV. Loss analysis

After analysing the RMS currents and proportional constants of key components, an experimental circuit was built to compare internal losses in the interleaved switching rectifier.Table 2 presents the electrical specifications of the switching rectifier. The input voltage ranges from a minimum of 110V to a maximum of 264V, the output voltage is 390V, with a maximum output power of 390W, and the switching frequency is fixed at 100 kHz. Table 3 lists the models and electrical characteristics of the main components used in the experimental circuit.Fig.3 shows the measured input voltage and current at input voltages of 110V and 220V, respectively. Fig.3 depicts the waveforms of the two switch voltages and the inductor currents measured during steady-state operation. As observed in Fig.3, the experimental circuit exhibits input voltage and current waveforms with similar shape and phase, consistent with the design intent of the switching rectifier described earlier. Sinusoidal current control reduces harmonic distortion and boosts power factor for improved efficiency.Notably, the two switches operate with a 180-degree phase difference, causing the two inductor currents to also be 180 degrees out of phase. This characteristic is typical of interleaved switching rectifiers, where the two independent inductor currents overlap at the input side, resulting in a reduction of current ripple. Such behavior positively influences the electrical characteristics by decreasing the ripple current, thereby improving the efficiency and reliability of the power conversion system. This study evaluated losses and efficiency of the interleaved switching rectifier using RMS equations and proportional constants from Table 1, which relate to output current.Initially, by maintaining a constant input voltage and varying the load current, the internal power losses could be expressed according to the proportional constants, reflecting the load characteristics. The results were then depicted in graphs. Fig.4 shows measured and calculated internal losses versus load current at 110V and 220V input.The measurement instruments used in the experiments, along with their specifications, are listed in Table 2. The results show that the measured internal losses generally exhibit similar characteristics across the load range when compared with the experimental data. Fig.4 illustrates the power conversion efficiency as a function of load current at input voltages of 110V and 220V. The experimental results and theoretical predictions from the loss analysis exhibit comparable trend patterns. From these findings, it can be inferred that the loss and efficiency analyses presented in this paper are valid within a certain range in practical experimental circuits. Moreover, if the internal parameters of key components reflected in the internal loss calculations are adjusted in advance, it would be possible to predict the contributions of individual components to overall losses and efficiency. This would facilitate the selection of components and the optimization of circuit design, leading to more effective and optimal design outcomes.

Table 2: Specifications of switching rectifier

Parameters	Normal	Minimum	Maximum	unit
Input voltage	220	110	264	V_{rms}
Output voltage	390	360	400	V_{DC}
Output power	-	10	390	W
RMS Input current	-	0.1	3.78	A_{rms}
Peak input current	-	0.14	5.34	A_{peak}
Switching frequency	100	30	100	kHz

Table 3: Specifications of key components

Parts		Model	Spec.	R(Ω)
Bridge Diode	BD	GBU805	400V 8A	
switch	S	IPP60R250CP	650V 25A	0.20
diode	D	C3D10060G	600V 10A	0.04
inductor	L	7804-09-0014	327uH	0.08
capacitor	C	LS Materials	450V	0.30

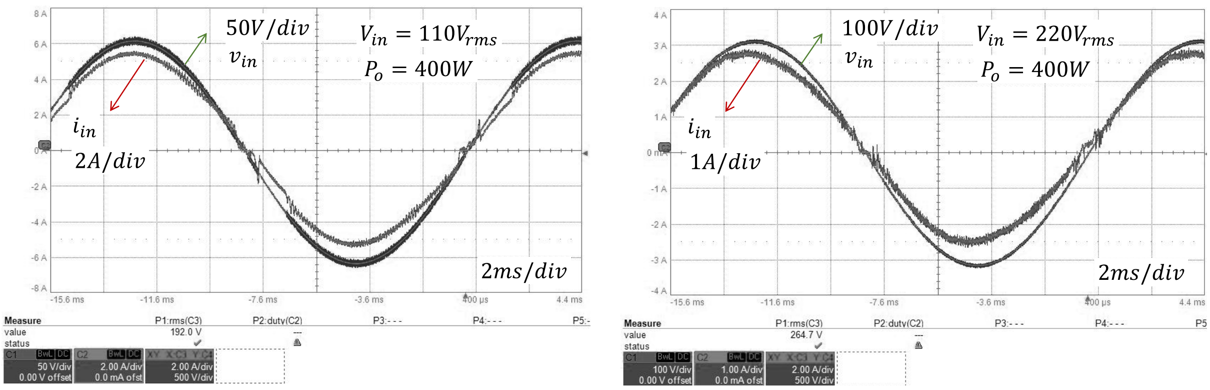

Fig.3: Waveforms of input voltage and input current

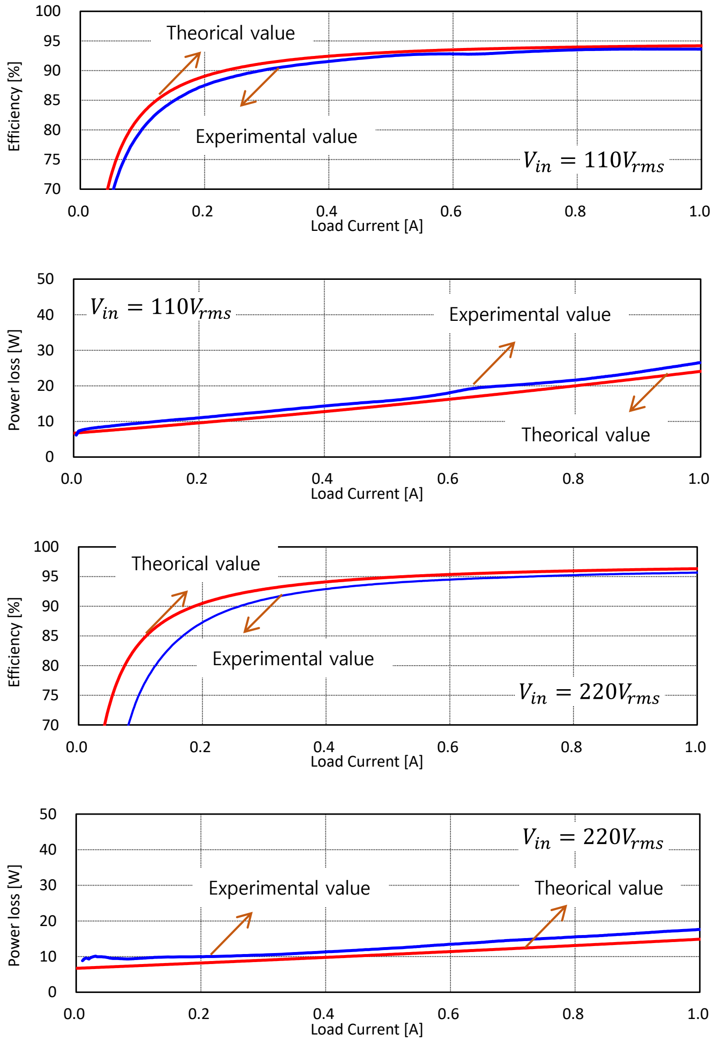

Fig.4: Power conversion efficiency and internal power loss

V. Conclusion

This paper proposes a systematic method to improve losses and efficiency through loss and efficiency analysis of an interleaved switching rectifier, a type of switching rectifier circuit with AC input. First, the RMS values of the key components' currents operating in steady-state conditions were derived, and these results were classified into three proportional constants based on their weighted contribution to the output load current. Using these results, it is possible to analyze the internal power losses associated with increasing load currents while maintaining a constant and fixed input voltage. To verify the validity of the loss analysis method, an experimental setup of an interleaved switching rectifier with approximately 400W power rated was constructed, and the experimental results were compared with the theoretical calculations. The results showed that across the entire load range, the theoretical and experimental values exhibited similar trends and were within a practical level suitable for active utilization during actual design stages. Therefore, the loss analysis process performed in this study demonstrated its validity for assessing internal power losses and power conversion efficiency, confirming its usefulness in the design and optimization of interleaved switching rectifiers.

References

[1] D. Zhou, X. Yu, and Z. Lu, High-Efficiency Interleaved Resonant Converters for Renewable Energy Systems, *IEEE Journal of Emerging and Selected Topics in Power Electronics*, *9(3)*, 2021, 3456-3467.

[2] Y. Wang, J. Zhang, and L. Qu, Impact of Parasitic Components on Loss and Efficiency of Interleaved Converters, *IEEE Transactions on Power Electronics*, *37(2)*, 2022, 1234-1245.

[3] C. Zhao, S. Wang, and X. Wu, Thermal Management and Loss Reduction Techniques for Interleaved Power Modules, *IEEE Transactions on Industrial Electronics*, *69(1)*, 2022, 123-134.

[4] J. Li, Y. Zhao, and Q. Lei, A Systematic Approach to Loss Modeling and Optimization of Interleaved Converters, *IEEE Transactions on Power Electronics*, *38(1)*, 2023, 234-245.

[5] K. Kim, S. Lee, and J. Choi, Efficiency Enhancement of Interleaved Converters Using Adaptive Dead-Time Control, *IEEE Transactions on Industrial Electronics*, *70(2)*, 2023, 345-356.

[6] L. Zhang, Y. Wang, and J. Li, Design and Implementation of High-Efficiency Interleaved Converters for Data Centers, *IEEE Journal of Emerging and Selected Topics in Power Electronics*, *11(4)*, 2023, 456-467.

[7] M. Chen, Q. Zhang, and X. Liu, Performance Evaluation of Interleaved Converters With Different Modulation Schemes, *IEEE Transactions on Power Electronics*, *39(1)*, 2024, 567-578.

[8] S. Kumar, R. K. Singh, and S. Mishra, Loss Analysis and Optimization of Interleaved Converters for Electric Vehicle Charging, *IEEE Transactions on Industry Applications*, *60(2)*, 2024, 678-689.

[9] H. S. H. Razavi, A. Radan, and M. F. Kangarlu, A Comparative Study of Interleaved Topologies for High-Voltage Power Conversion, *IEEE Transactions on Power Electronics*, *40(3)*, 2025, 789-800.

[10] Y. Xu, Z. Wang, and X. Li, Advanced Control Techniques for Improving Efficiency and Power Density of Interleaved Converters, *IEEE Transactions on Industrial Electronics*, *72(1)*, 2025, 890-901.

[11] Q. Lei, J. Sun, and Y. Zhao, Design and Analysis of High-Frequency Interleaved Converters With Integrated Magnetics, *IEEE Journal of Emerging and Selected Topics in Power Electronics*, *13(1)*, 2025, 901-912.